Influence of different design parameters on a coplanar capacitive sensor performance*

Farima Abdollahi-Mamoudan[a,*], Sebastien Savard[b], Clemente Ibarra-Castanedo[a], Tobin Filleter[c] and Xavier Maldague[a,**]

[a]*Department of Electrical and Computer Engineering, Université Laval, 1065 Avenue de la Médecine, Québec, QC G1V 0A6, Canada*
[b]*Eddyfi Technologies, 3425, av. Pierre-Ardouin , Québec, QC G1P 0B3, Canada*
[c]*Department of Mechanical and Industrial Engineering, University of Toronto, 5 King's College, Toronto, ON M5S 3G8, Canada*

ARTICLE INFO

Keywords:
Capacitive sensor
NDT
Coplanar electrodes
Finite element modelling

ABSTRACT

Coplanar capacitive sensors are employed in Non-destructive Testing (NDT) methods to measure the difference in dielectric properties of the materials. The most important design parameters for a coplanar capacitive sensor include the shape, size, and separation distance of the electrodes which affect the sensor performance. In addition, the impact of the shielding plate and guard electrode should be considered. In the framework of this paper, numerical simulations and physical experiments are studied for two shapes of electrodes, triangular and rectangular, by examining different sizes and different separation distances between electrodes to assess and analyze the important features of the coplanar capacitive electrodes, such as the penetration and strength of the electric field as a function of sensor geometrical properties. Therefore, a detailed analysis of numerical simulation using Finite Element Modelling (FEM) is provided to study these geometric parameters. In addition, the influence of the different frequencies, lift-off, and the presence or absence of a metal shielding plate and guard electrode on the output result is analyzed. Finally, sensors were manufactured and several experiments were carried out under different configurations. Comparison of the numerical simulation results and physical experiments illustrate that they are in good qualitative agreement.

1. Introduction

Non-Destructive Testing (NDT) refers to the process of evaluating and inspecting materials to identify or detect defects in comparison with some standards without changing the main features or causing damage to the tested object [1]. To select the most appropriate NDT method, there should be information about the material and test conditions. First, the exact type of material of the specimen should be specified (conductive or non-conductive and the constituent compounds of each). Second, the shape of the specimen should be considered (flat, pipe, weld, gear, etc.). Third, it should be determined what type of defects are of interest (cracks, delamination, impact damage, corrosion, porosities, etc.). Fourth, the size of the defects that are expected should be known to some extent (very small indications or large defects). Fifth, the location (surface, far side or subsurface) and the direction (parallel or perpendicular to the surface) of the expected defect should be known. Lastly, the condition of the surface of the specimen (painted, coated, rusty or rough) and the condition of the environment of the experiment (dusty, radioactive, underwater, etc.) should be specified. Thus, the type of materials (conducting or non-conducting), advantages and disadvantages of the NDT method, and also the financial constraints of the method should be considered in order to choose a proper NDT technique. Accordingly, a certain form of energy based on the chosen NDT method is transferred to the specimen, this energy alters due to the existing defect and returns to the instrument. Consequently, the inspector can retrieve significant information about the specimen [2].

There are several types of NDT techniques that are commonly used in both industrial applications and scientific research areas. However, ultrasonic testing (UT), infrared thermography (IRT), radiography testing (RT), and eddy current testing (ECT) are among the most common [3, 4]. Although each of them has its own advantages for investigating material, the choice of one or the other depends on the inherent limitations of each method, to name only a few: UT requires contact and the use of a coupling medium (gel or water); in IRT the effect of the surrounding environment (radiation) and an uneven or low emissivity of the surface may limit its use; RT suffers from radiation exposure problems and requires access to both sides of the inspected object; and ECT is limited to electrically conductive materials [1]. Therefore, a new NDT method is required to overcome some of the restrictions associated with other techniques.

Capacitive sensing or Capacitive imaging could be considered as a comparably new NDT technique since it was first introduced only recently in 2006 as an NDT method [5]. The mechanism of this method is relatively simple. The

* This research is funded by the Natural Sciences and Engineering Research Council of Canada (NSERC) - Discovery Grant Program, the Candian Foundation for Innovation (CFI), Canada Research Chair Program, NSERC CREATE « oN DuTy! », MITACS.

*Corresponding author
**Principal corresponding author
farima.abdollahi-mamoudan.1@ulaval.ca (F. Abdollahi-Mamoudan); ssavard@eddyfi.com (S. Savard); clemente.ibarra-castanedo@gel.ulaval.ca (C. Ibarra-Castanedo); filleter@mie.utoronto.ca (T. Filleter); xavier.maldague@gel.ulaval.ca (X. Maldague)
ORCID(s): 0000-0003-0158-0839 (F. Abdollahi-Mamoudan); 0000-0002-0198-7439 (C. Ibarra-Castanedo); 0000-0003-2609-4773 (T. Filleter); 0000-0002-8777-2008 (X. Maldague)

parallel plates of the regular capacitor generate a uniform electric field distribution when a voltage is applied between them. By changing the position of these plates, the electric field distribution changes and a fringing electric field is created. This fringing field expands into the specimen and can be monitored for NDT purposes [6]. Figure 1 illustrates a schematic diagram of changing the position of the plates from parallel to coplanar and how the electric field distribution changes due to these variations. The opposite charges are created on the coplanar electrodes when they are connected to a power supply. These charges attract each other, and an electric field is generated as the charges build up [7].

The principle of this method consists of placing two (or several) electrodes on the surface of the specimen and then applying an AC voltage between them. The basic diagram of a coplanar capacitive sensor over a sample is shown in Figure 1c. This system operates as a capacitor and capacitance variations may illustrate the presence of interior structure (such as a defect) [8, 9]. It is especially a potential method to evaluate and characterize the dielectric properties of non-conducting materials such as glass fibre reinforced polymer (GFRP). The dielectric constant or permittivity is one of the dielectric properties of materials, which provides a measure of the material's capability of storing electric energy [2]. Assuming that the material under test and a defect have different permittivity values, the electric field distribution will change due to the presence of the defect. Electric field distortion causes a change in the charge induced in the sensing electrode, and this change in the charge can be identified and used for detecting defects [10].

An example of the electric field distortion due to the presence of defects has been demonstrated in the previous paper [9]. According to this example, defects cause a perturbation in the electric field distribution due to the various dielectric properties (such as permittivity) of the specimen and defects, leading to changes in the detectable signal. Thus, material dielectric properties, as well as the electrode geometry affect the capacitance between the two electrodes [11]. The difference between the permittivity of the material and the defect leads to the electric field distortion and hence the variation of the potential on the sensing electrode [12]. Accordingly, the model shows how the capacitive sensor detects the flaws and can be used for the NDT of the materials.

Capacitive sensing possesses some advantages compared to other NDT methods and is broadly applied to the range of applications due to the low cost, fast response, non-invasive, no radiation, no need coupling medium, and flexibility in the design of the electrodes [10, 13]. Furthermore, the coplanar sensor requires single-sided access to the material and this is one of the most important advantages of this method, especially when accessing both sides of the specimen is restricted [6]. This method has the potential to detect corrosion under insulation (CUI) [14–16], rebar in concrete [10, 17], water intrusion into composite structures [8, 18], cracks, and delamination of the material [10], impact damage [10, 19], surface defects in conductive materials [5, 20] and carbon fibre composites [10]. In addition, capacitive sensor manufacturing is relatively straightforward and there is no need to use expensive equipment or complex operating procedures to achieve sought inspection results [7]. These features of the coplanar capacitive sensor make it an interesting method for applications in non-destructive testing [3], material characterization [21] and imaging [22, 23]. In addition to observing a good agreement between capacitive imaging and ultrasonic phased array on CFRP panels containing impact damage [19], it has some advantages over ground penetrating radar (GPR) for a cover concrete to an adjustable depth [8]. Similar to all other NDT techniques, this method has some drawbacks. For instance, the method is sensitive to the air gap between the surface of the electrodes and sample (in comparison to the size of the electrodes) [24] and it cannot detect the sub-surface flaws in metals.

The coplanar capacitive probe performance is primarily determined by its electrodes geometry. It can be simple and named "symmetric geometry", such as a pair of triangular, square, and rectangular or complex forms like the comb shape. Another common geometry is named "Concentric geometry" which may contain a central disc and several outer annuluses as the main electrodes and guard electrode or may simply contain several rings [25]. In addition, the size of the electrodes, the separation distance between them, the shielding plate and guard electrode are the essential parameters for evaluating the performance of a capacitive sensor since they have a great impact on the penetration depth and the electric field strength which are the most important factors to consider when assessing a capacitive sensor performance [26]. The penetration depth, which is one of the most important factors to evaluate the performance of the coplanar capacitive probe, is defined as the maximum distance in the vertical direction to the surface of the specimen that leads to detectable changes in the sensor output and shows how deep the sensor can indicate the characteristics of the material [6]. Therefore, it is important to determine the influence of each parameter on the sensor performance in order to achieve an optimized sensor and desired results.

Several studies have been carried out on the main parameters of the coplanar capacitive sensor in various forms. Although they were able to answer some of the ambiguities about the influences of these parameters, all parameters were not considered for one specific shape of the electrode individually. For instance, in [18], the effect of the electrode width and the separation distance between them for a pair of rectangular electrodes was investigated by the finite element method. This model was restricted to two dimensions (2D) and the electrode length effect was not taken into consideration (electrodes were assumed to be of infinite length). In addition, the impact of the shielding plate and guard electrode were not considered in this model. In [27], two different sizes of equilateral triangular electrodes were considered to assess the effect of the electrode size. However, the impact of the separation distance between the driving and sensing electrodes was not considered individually and neither was the effect of the shielding plate. In [26], the impact of the separation between the centroid of a pair of square

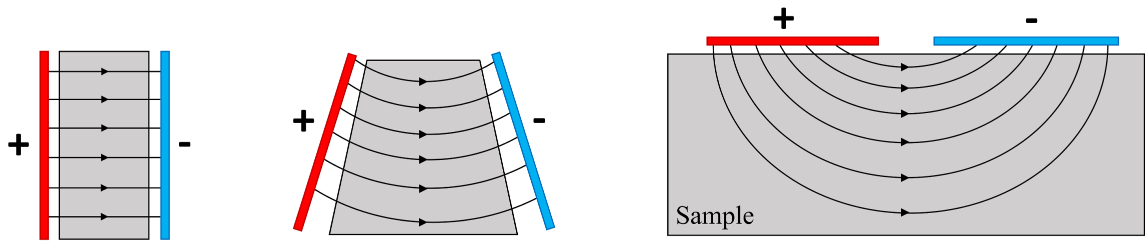

Figure 1: Schematic diagram of the electric field distribution as electrodes turns from a parallel geometry of the capacitor (left) to coplanar (right): (a) Parallel-plate capacitor, (b) electrodes open up, and (c) one-sided access to the sample.

electrodes, the effect of a guard electrode for a pair of rectangular electrodes, and the effect of the shielding plate for a pair of a triangular electrode were studied. However, the impact of the electrode size was not considered in this paper. In [28], the effect of different sizes of the triangular shape was investigated for three probes, while the separation between the electrodes was kept constant. Thus, the impact of this parameter was not studied. In [12], three pairs of triangular probes with different areas were studied. However, the effect of the electrode size and the separation between them has not been investigated individually. It is thus useful to investigate the effect of each parameter (such as the size of the electrodes, the separation between them, the shielding plate, and the guard electrode) individually for a specific geometry of the coplanar capacitive sensor. These parameters have been studied for the concentric geometry in [6] and [26].

In this paper, the effect of the various frequencies on the electric field strength and penetration depth for a coplanar capacitive sensor was investigated by a three-dimensional Finite Element Model (FEM) in COMSOL Multiphysics software which has not been demonstrated in the previous works. Two of the most widely used electrode shapes based on the literature, the triangular and rectangular shapes, were selected to study the impact of the electrode shape on the sensor performance. The advantages of the rectangular probe were illustrated, and then, the other design parameters such as the shielding plate, guard electrode, electrode size, and the separation distance between the electrodes were considered and fully described to assess their effect on this specific geometry (rectangular shape) through FEM simulations. In addition, the effect of the lift-off on the penetration depth and electric field strength was shown. It was concluded that the existence of a shielding plate and guard electrode, and increasing the electrode size as well as the separation distance between the electrodes increases the penetration depth. These results were validated by physical experiments and it was demonstrated that the penetration depth and output signal changed with respect to the shape, size, and separation distance of the electrodes in agreement with experimental data. Therefore, in this paper, in addition to studying the effect of frequency, all design parameters for the rectangular probe were investigated for the first time.

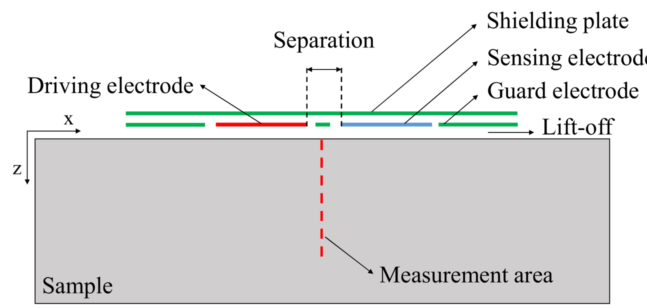

Figure 2: Side view of the sample and the coplanar capacitive sensor with shielding plate and guard electrode, and the centerline as a measurement area.

2. Numerical simulations

There are several parameters in the design of the sensor which should be considered when evaluating its performance. The efficiency and performance of a capacitive sensor are primarily determined by its shape, size, and separation distance between the driving and sensing electrodes. In addition, the effect of the shielding plate and the guard electrode should not be neglected. Each of these factors may affect several aspects of the sensor performance. Therefore, awareness of design factors is important to achieve the desired sensor performance and optimize the sensor for a particular application [29]. In this paper, the effect of each parameter is evaluated by a three-dimensional (3D) FEM. Moreover, the effect of frequency and lift-off are considered. FEM is a useful tool for predicting the fields created by coplanar capacitive electrodes and how these fields are likely to interact with different materials and defects. Theoretical simulation models were conducted using the COMSOL™ Multiphysics FE package, the AC/DC module, which can be used to model the predictions of the design parameters influence on the output and to optimize the design of the sensor. Since the effect of the electromagnetic field is minimum and negligible in this study, a quasi-static approximation has been used.

2.1. Simulation setup

As depicted in Figure 2, a coplanar capacitive probe is composed of: (1) a driving electrode (the red one) and sensing (the blue one) electrode, (2) a shielding plate, and (3) a guard electrode. In this study, a pair of coplanar electrodes are placed above the surface of a non-conducting sample, and the computational domain was assumed to be filled with air and the relative permittivity was set to 1.0. The material of the insulating substrate of the sensor was flame retardant woven glass-reinforced epoxy resin (FR-4) with 0.5 mm thickness, and accordingly, the relative permittivity was set to 4.4 [30]. The conducting shielding plate, if used, is on the top of the substrate and was held in ground potential, while the driving electrode was excited with an amplitude voltage of 10 V. To inspect the sensor response in relationship with the design parameters, the measurements were against the variable in the evaluation and taken along a centerline between the two electrodes, as shown in Figure 2. A user-controlled mesh was used and the mesh generation density was set to be “Finer” for the airbox (since it has less impact on the result) and “Extra Fine” for the electrodes and sample. The approach taken by 3D COMSOL Multiphysics is to divide the various materials and geometries into triangular elements and to represent the electric field within each element with a separate polynomial. The electric field strength can be retrieved from FEM and analyzed since the electric field lines (E) and the electric potential (V) are perpendicular to each other [16, 31]. Therefore, all of the simulation results are based on the electric field strength and can easily be compared to the experimental results.

2.2. Frequency

The electric field strength versus penetration depth by different excitation frequencies was studied while keeping all other parameters constant in order to investigate the effect of the excitation frequency on the penetration depth and electric field strength when used with a non-conducting material. In Figure 3, the horizontal axis is the vertical distance from the sample surface up to 10 mm below it (the red dash-line in Figure 2). Based on this, for 0.1 kHz frequency, the electric field strength will be reached zero by 6 mm depth, or for 1.0 kHz frequency, the electric field strength is close to zero after 7 mm depth and the other frequencies have approximately the same behaviour after 7 mm depth, and will be closed to zero after 9 mm. And, when the electric field strength becomes zero, there will be no more output. Therefore, these variations cause small differences in penetration depths.

By comparing the results in Figure 3, it can be inferred that the changes in frequency in a limited range (from 0.1 to 200 kHz) lead to variation in both penetration depth and electric field strength. It can be observed that both the penetration depth and electric field strength of 0.1 kHz appears to be much less than that of the other frequencies (and may not generate acceptable results), and frequency of 10, 100, and 200 kHz have almost a similar impact on the sensor performance.

The capacitive technique is different from other electromagnetic NDT methods such as eddy currents where the penetration depth is governed by the frequency of the input signal. Although the frequency is not a major factor for assessing the capacitive sensor performance and does not have a significant effect on the penetration depth (from 10 to 200 kHz), it affects the electric field strength in a limited range. The frequency also depends on the properties of the material under inspection such as the respective electrical conductivity, and the instrument which is used for the experiment.

Based on the simulation results in Figure 3, it can be seen that as the frequency increases, the electric field strength in the specimen also increases up to a frequency of 10 kHz, after which, no significant differences in the sensing depth and electric field can be observed. Since the curves at 100 and 200 kHz show only small differences in the electric field and cause the most strength of the electric field and penetration depth, a frequency of 100 kHz is considered for all other simulations.

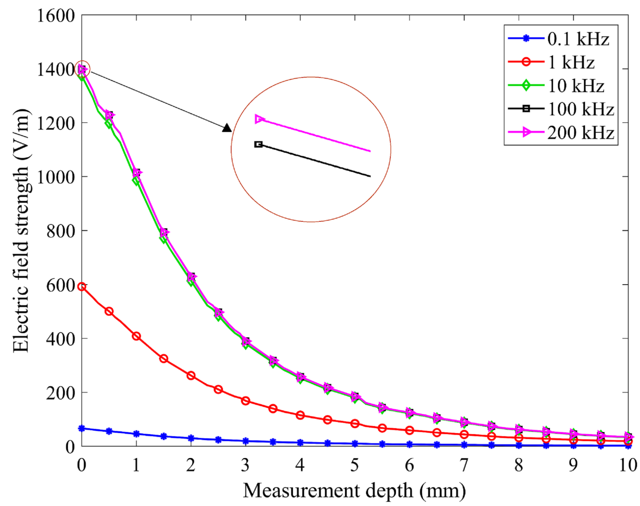

Figure 3: Simulation results showing Electric field strength vs. Depth. Measurements were taken along a centerline between the electrodes by varying the frequency. The frequencies are 0.1, 1.0, 10, 100, and 200 kHz.

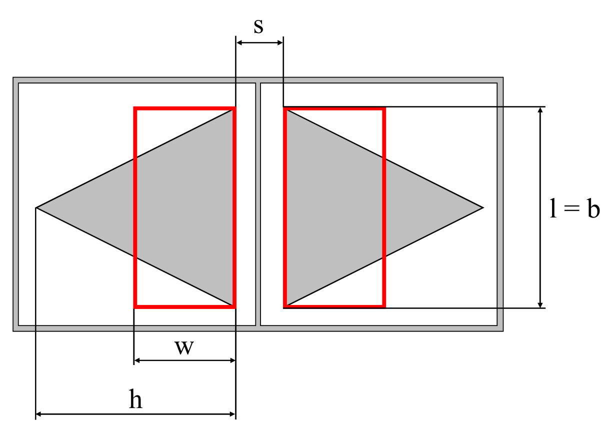

Figure 4: Diagram of a pair of rectangular and triangular coplanar electrodes with equal area, equal separation distance, and equal close edge.

2.3. Electrode shape

The shape of the electrodes is an important factor in the design of the capacitive sensor which has a significant effect on the sensor performance. As mentioned in the introduction section, a triangular and a rectangular probe with the same area of the electrodes and the same separation distance between them were simulated to compare their performance. To make a direct comparison and assess the impact of the two close edges of the electrodes, the base (b) of the triangle is equal to the length (l) of the rectangle, l = b, and the height (h) of the triangle is twice the width (w) of the rectangle, h = 2 w, as indicated in Figures 4. The separation between electrodes in both geometries is s. According to the simulation results which are shown in Figure 5, it can be concluded that both shapes of electrodes have approximately the same penetration depth, although the electric field strength is slightly higher for the rectangular probe. This conclusion has also been confirmed in the experimental results section. In addition, if there are two defects close together, each defect will affect the electric field distortion of the other defect, and this may lead to inappropriate results for the main defect and might cause errors in measurements. The impact of this situation, for a rectangular probe is much less and even negligible. This is demonstrated by numerical simulation in Figure 6 and 7 for the rectangular and the triangular probe, respectively. These figures show a surface plot for two different views of the simulation: (a) is the top view (the *xy* plane), and (b) is the side view (the *xz* plane) of the simulations. It is obvious that for the triangular probe the presence of defect 2 distorts the electric field line which will affect the output of defect 1. However, for the rectangular probe, the presence of defect 2 has a negligible effect on the output when scanning defect 1. This can be seen more clearly in Figure 8 which presents a contour plot of the electric field distribution. Although defect 2 for the rectangular probe distorts some of the electric field lines, these lines are not in the high sensitivity region. Therefore, a pair of rectangular electrodes is suggested where there is a restriction of the overall size of the capacitive sensor. Rectangular electrodes are especially beneficial when a multi-electrode capacitive sensor is required. It is worth noting that, with the purpose of maintaining the same area on both electrode geometries for comparison purposes, the triangular-shaped probe has a larger height than the width of the rectangular one (as seen in Figure 4), which leads to a larger area coverage in the direction of the height and the eventual interference of the triangular sensor with defect 2.

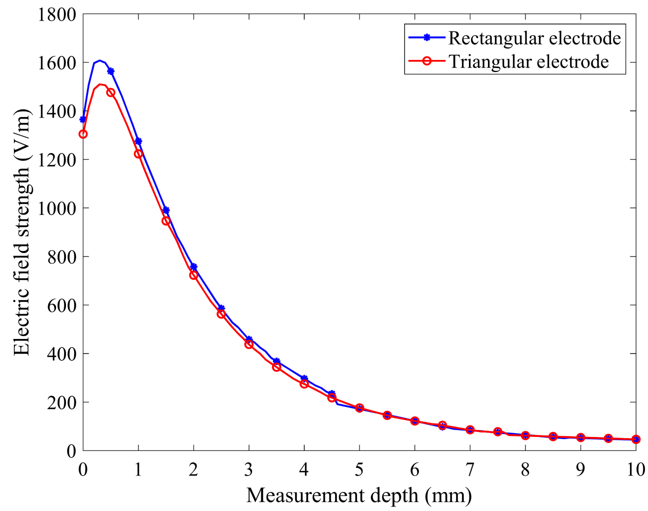

Figure 5: Simulation results showing Electric field strength vs. Depth. Measurements were taken along a centerline between the electrodes for a pair of rectangular and triangular coplanar electrodes with equal area, equal separation distance, and equal close edge.

2.4. Shielding plate

The effect of the parasitic field of the surrounding environment is one of the main challenges of using capacitive sensors. The proximity of the electrical conductor's components to each other or to circuits leads to parasitic capacitance or stray capacitance due to their different voltages. The difference in the voltage creates an electric field distribution between them and leads to an electric charge being stored on them. This parasitic capacitance is unavoidable and usually unwanted and should be minimized as much as possible. A shielding plate can minimize the undesirable electric fields, eliminate stray capacitance and noise from an unwanted area in the sensing region, and steer the electric field lines mainly in the direction of the sample [6].

The effect of the presence of a conducting shielding plate vs. the absence of one on the penetration depth and electric field strength was investigated using FEM for a pair of rectangular electrodes. Figure 9 indicates the simulation results showing this effect. As can be observed, the use of a conducting shielding plate above the substrate increases the penetration depth, however decrease the electric field strength. It can also be found that the electric field strength variations with the depth are more important at shallow depths (for defects at less than 1 mm) and much less pronounced for deeper defects (for defects at 2 mm and deeper). This is because the shielding plate absorbs the electric field lines from the main electrodes, which will lead to a weaker electric field. However, the benefits of using a shielding plate overcome this reduction in electric field strength since it can significantly reduce the impact of parasite capacitance and unwanted fields from the ambient. The shielding plate is placed on the backside of the main electrodes and is usually held in the ground potential.

2.5. Guard electrode

The role of the guard electrode is to prevent the electric field lines from directly reaching the sensing electrode, by forcing them to pass through the sample to reach the sensing electrode, thus the penetration depth will increase. In addition, a guard electrode is needed to decrease the noise from other sources and to prevent the direct coupling between driving and sensing electrodes. Usually, the guard electrode is held at ground potential [26]. The effect of the

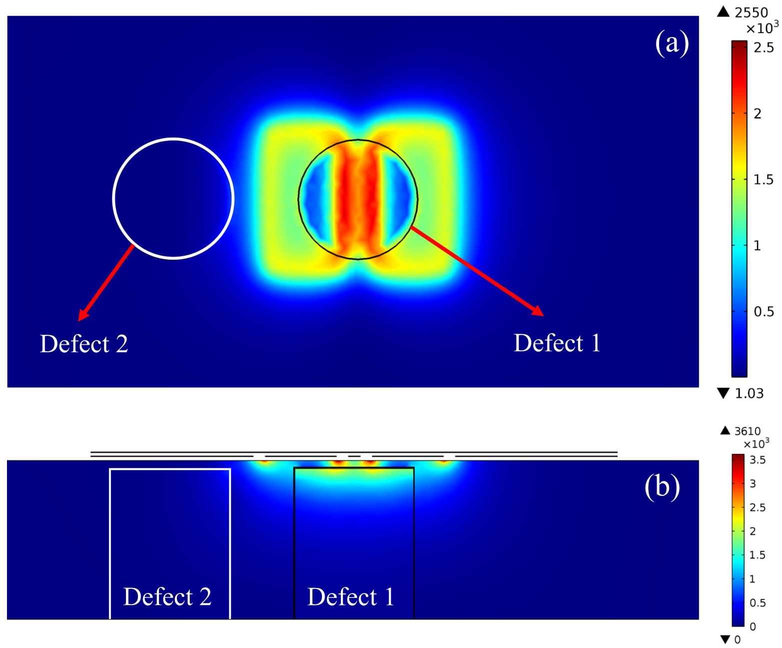

Figure 6: Simulation results showing a surface plot of the electric field distribution (V/m) for the rectangular probe over a sample with two defects. The simulations are in different planes: (a) the *xy* plane (the top view) and (b) the *xz* plane (the side view).

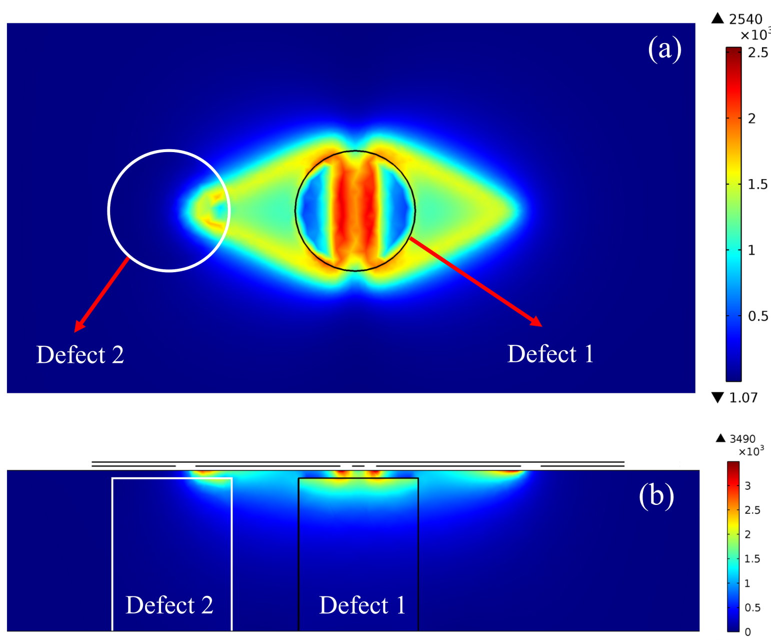

Figure 7: Simulation results showing a surface plot of the electric field distribution (V/m) for the triangular probe over a sample with two defects. The simulations are in different planes: (a) the *xy* plane (the top view) and (b) the *xz* plane (the side view).

presence of a guarding electrode on the penetration depth and electric field strength was studied for the same pair of rectangular electrodes. From the results in Figure 10, it can be concluded that the grounded guard electrode causes a deeper penetration depth since the grounded guard electrode restricted the electrical field within a narrower range and prevented the field lines from going directly from the driving electrode to the sensing electrode. This causes the electric field to move towards the tested material and increases the penetration depth. However, the guard electrode reduces the electric field strength since it absorbs the electric lines from the main electrodes, which causes a weaker electric field.

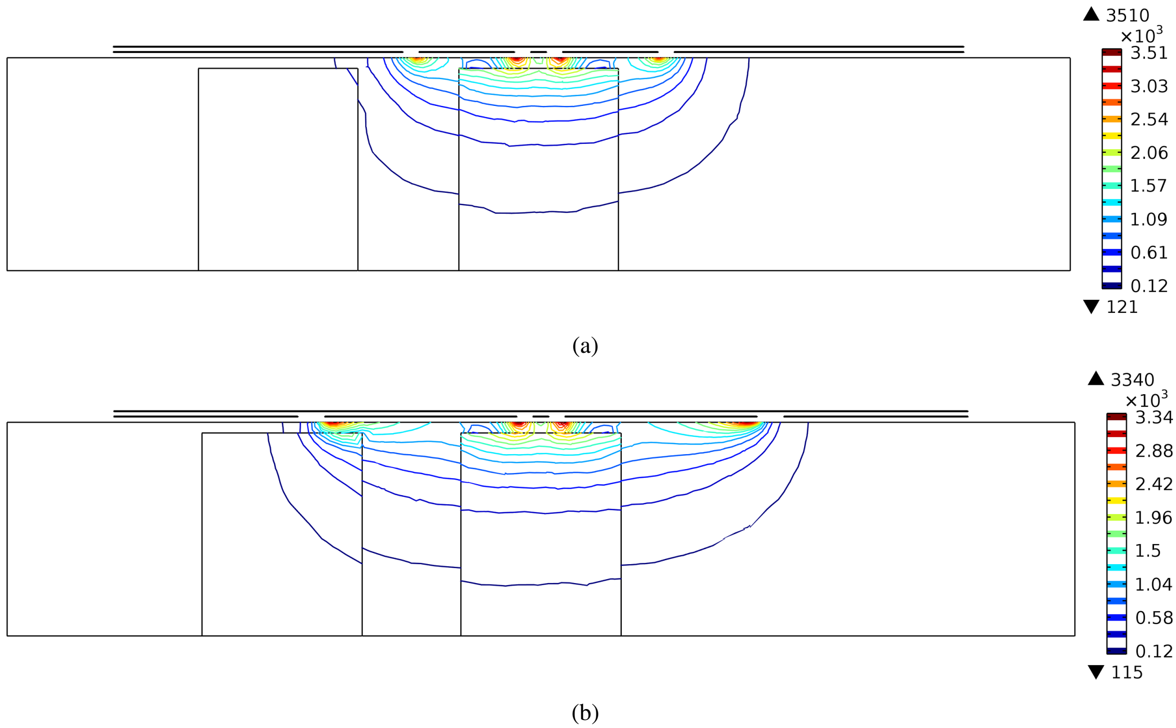

Figure 8: Simulation results showing a contour plot of the electric field distribution (V/m) in a sample containing two defects in the *xz* plane: (a) the rectangular probe and (b) the triangular probe.The sensors have an equal area, equal separation distance, and equal close edge.

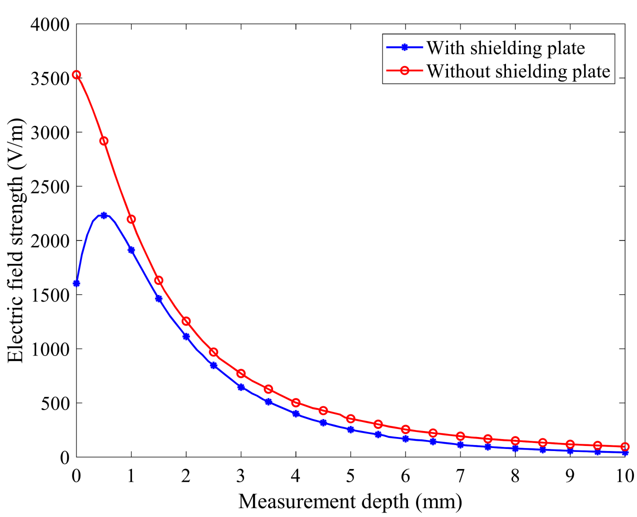

Figure 9: Simulation results showing Electric field strength vs. Depth. Measurements were taken along a centerline between the electrodes with and without the shielding plate.

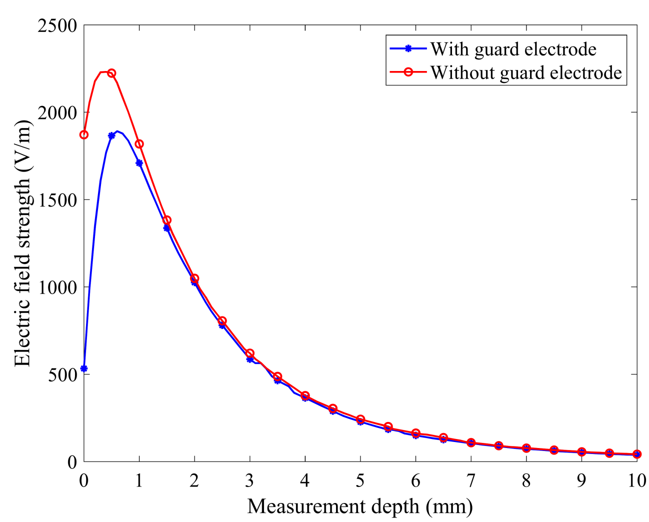

Figure 10: Simulation results showing Electric field strength vs. Depth. Measurements were taken along a centerline between the electrodes with and without the guard electrode.

2.6. Electrode size

One of the main design parameters for the capacitive sensor is the electrode size and it is different for various applications. On one hand, small electrodes are not appropriate for scanning large defects. On the other hand, large electrodes are not sensitive enough for scanning defects considerably smaller than their size. Generally, larger electrodes can reach a deeper penetration depth and a greater signal strength, although, in imaging applications, the image resolution decreases since the sensor takes a sample of a larger volume [27]. It is worth noting that in the capacitive sensor design maximizing the signal to noise ratio is one of the most important issues [7]. Therefore, the size of the electrodes should be carefully chosen to achieve the proper penetration

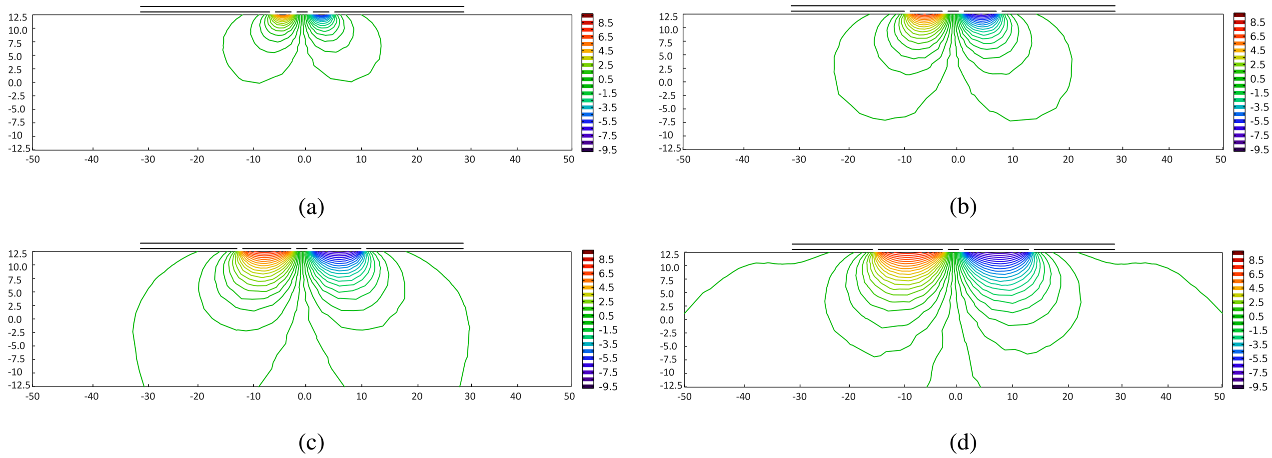

Figure 11: Simulations results showing a contour plot of the electric potential distribution (V) in the *xz* plane for the rectangular probe with different electrode widths: (a) 3, (b) 6, (c) 9, and (d) 12 mm.

depth and output signal for different applications.

According to Section 2.3, a pair of rectangular electrodes was selected in order to investigate the effect of the electrode size. The different widths of the rectangular electrode were considered as an element of the size effect on the electric field strength and the penetration depth while all other parameters were kept constant. Figure 11 shows an example of the increase of the inspected volume due to an increase of the electrode width. This figure depicts the contour plots of the electric potential for different widths of the electrodes in the *xz* plane. In addition, from the results of Figure 12, it is obvious that the electric field strength and the penetration depth increase with the width of the electrodes. However, w = 9 and 12 mm have approximately the same penetration depth (since the electric field strength maximum occurs at approximately the same depth, i.e. at a penetration depth around 1 mm), but the electric field strength is greater with w = 12 mm. This is confirmed by the experimental result shown later (Section 4.2) in this work. Therefore, there should be a trade-off between the output signal and sensing depth (the penetration depth of the electric field into the specimen) and the size of the sensor should be optimized based on the application. Furthermore, the constraint of the overall size of the sensor must also be considered.

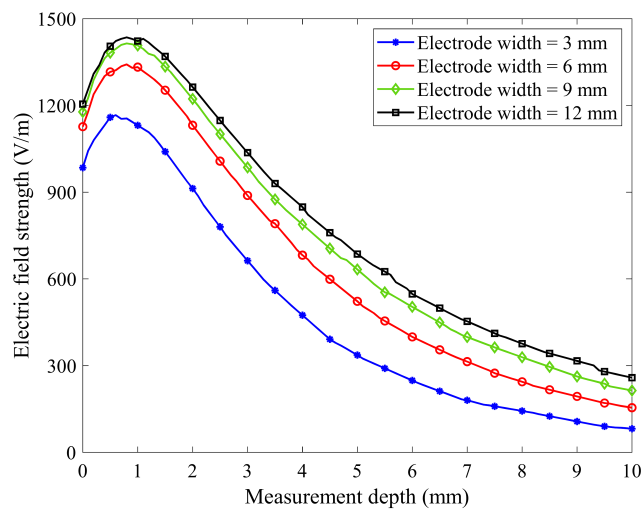

Figure 12: Simulation results showing Electric field strength vs. Depth. Measurements were taken along a centerline between the electrodes by varying the electrode widths.The widths are 3, 6, 9, and 12 mm.

2.7. Separation between electrodes

In a coplanar capacitive sensor, the separation between the driving and sensing electrodes is an effective element in controlling the penetration depth, electric field strength, and sensor performance. The separation between the electrodes refers to the distance between the edge of two adjacent electrodes, as shown in Figure 4. Generally, the penetration depth increases with the separation distance between electrodes since the electric field lines have to travel a greater distance into the sample to reach the sensing electrode [25]. The effect of this parameter on the sensor performance is studied by numerical simulation. Figure 13 illustrates the results of the simulations of the different separations between the driving and sensing electrodes while all other parameters are kept constant.

It can be seen that a greater penetration depth will be achieved due to the increasing separation between the electrodes. However, this reduces the electric field strength since the coupling between the driving and sensing electrodes is reduced due to the increasing separation between the electrodes. Reciprocally, a smaller distance between the electrodes produces more concentrated electric field lines at the sample surface which is beneficial for the detection of shallower defects. Therefore, there should be a trade-off between electric field strength and the depth of penetration to achieve a desirable performance.This is in good agreement with the experimental results.

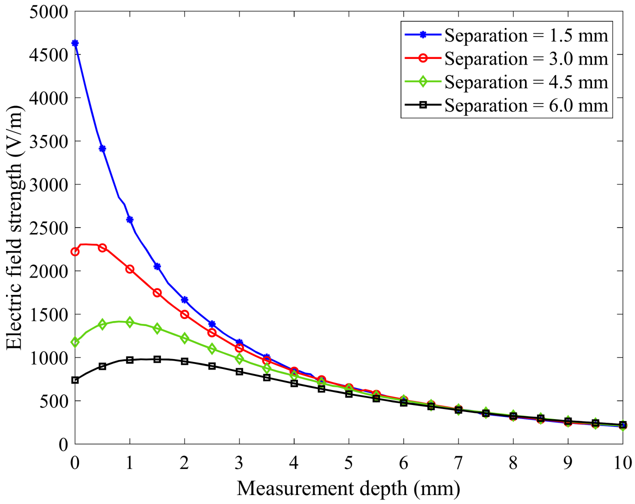

Figure 13: Simulation results showing Electric field strength vs. Depth. Measurements were taken along a centerline between the electrodes by varying the separation between the electrodes. The separation distances are 1.5, 3.0, 4.5, and 6.0 mm.

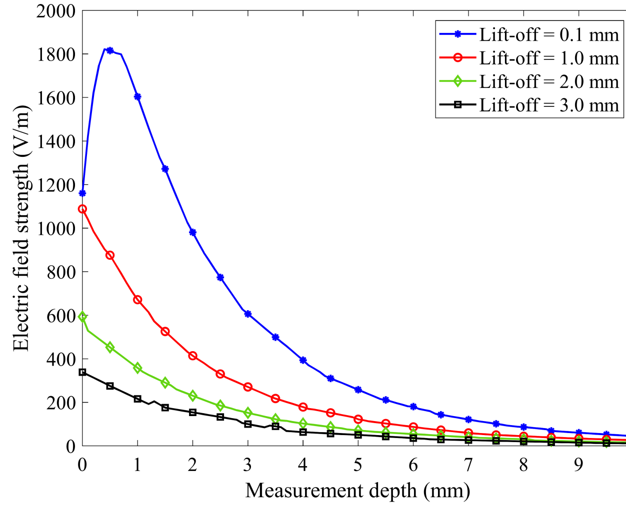

Figure 14: Simulation results showing Electric field strength vs. Depth. Measurements were taken along a centerline between the electrodes by varying the lift-off. The lift-offs are 0.1, 1.0, 2.0, and 3.0 mm.

2.8. Lift-off

For a coplanar capacitive sensor, the distance between the specimen surface and probe surface, referred to as lift-off, as shown in Figure 2, is one of the main barriers of this technique since a larger lift-off decreases the capacitance between the electrodes and hence reduces the output voltage. In addition, it reduces the extent of penetration of the electric field into the sample, which leads to a decrease in the depth of penetration [24].

To investigate the effect of lift-off on the sensor performance for a non-conducting specimen, FEM simulations were performed to identify the relationship between the electric field strength, penetration depth, and different lift-offs, while all other parameters are kept constant. From the simulation result in Figure 14, it can be inferred that the probe can reach a penetration depth of about 1 mm with a lift-off of 0.1 mm while the concentration of the electric field will decrease and occur at the surface of the specimen as the lift-off increases. This means that a large lift-off could prevent the detection of some defects (deep defects in particular) since the electric field strength variations with the depth will occur closer to the surface. Therefore, the coplanar capacitive sensors should always be kept at a minimum distance from the surface of a non-conducting sample to achieve the maximum electric field strength and depth of penetration.

3. Sensor manufacturing and experimental setup

The sensor manufacturing steps include the material selection for electrodes, the insulation layer for the surface of the electrodes, the back substrate of the electrodes, and the choice of a fabrication method. The electrodes are made of conducting materials such as copper. Non-conducting materials are used for the insulation layer and the sensor substrate. The insulation layer is very thin and is placed on the electrodes to prevent direct contact of the electrodes with the specimen. This prevents scratches on the electrode surface and the oxidation process of metal. The thicknesses of the insulation layer and the sensor substrate can affect the electric field strength and penetration depth, and thus need to be optimized.

In this paper, the capacitive sensor is fabricated on a double-sided printed circuit board (PCB). The main electrodes are surrounded by a guard electrode and all of them are made of copper and covered with a thin insulation layer (a Kapton tape with 10 µm thickness). The PCB was also coated in copper on its back surface as a shielding plate. A thin substrate with 0.5 mm thickness is applied in order to achieve a greater sensing depth and output voltage. The substrate is made of flame retardant woven glass-reinforced epoxy resin (FR-4), which is a commonly used material for PCB. Each of the main electrodes can be used as either a driver or a receiver. To generate an electric field distribution, one of the plates is used as a transmitter and connected to Ectane. Ectane is a multi-technology, powerful and compact instrument for generating and analyzing signals. This instrument generates the excitation signal to the sensor, and processes and digitizes the return signal from the sensors to be read into the acquisition and analysis software. The frequency range of this instrument is 5 Hz up to 10 MHz and the generator output is up to 20 V, peak to peak. A differential amplifier is placed inside Ectane to process the received signal successively. The output signal from the Ectane is proportional to the instantaneous value of the dielectric property of the material averaged over the field distribution within the material. To generate an electric field distribution in the material under test, the driving electrode was connected to the

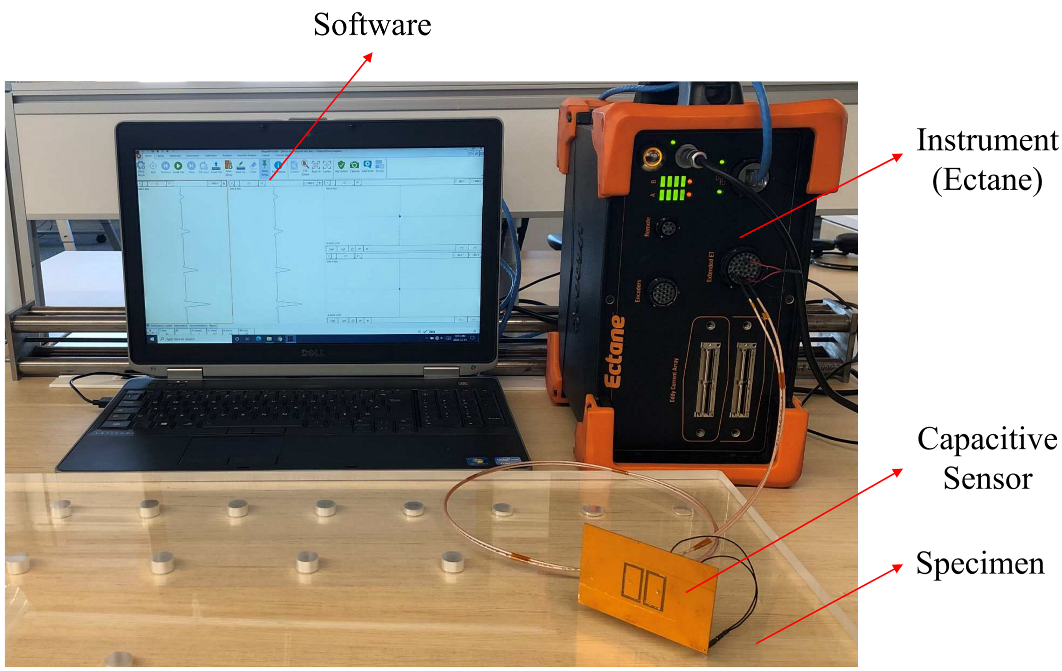

Figure 15: The experimental arrangement used for the capacitive sensing technique.

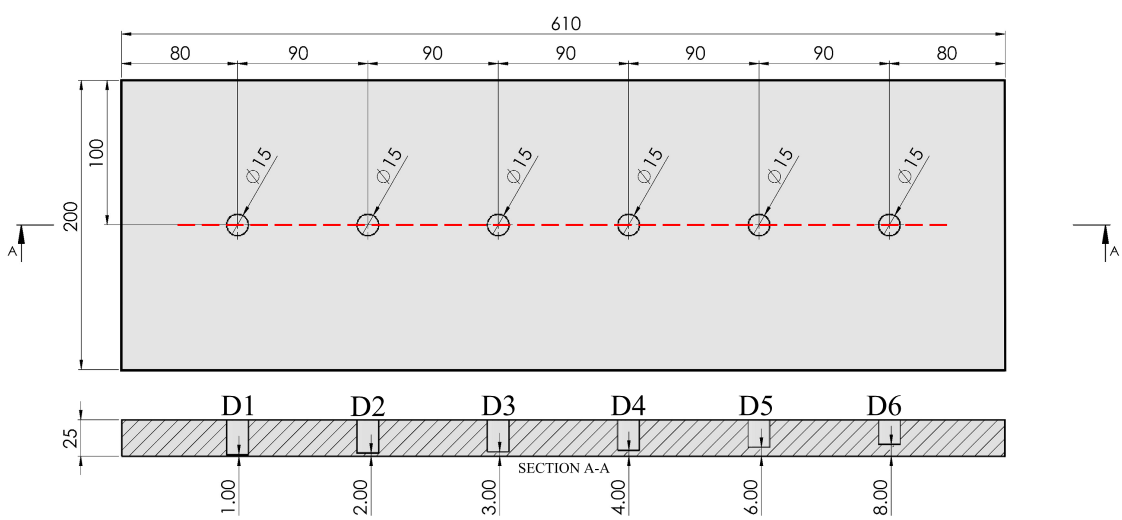

Figure 16: Schematic diagram of a 25 mm thick acrylic board containing flat-bottomed holes of buried depth (from left to right) 1, 2, 3, 4, 6, and 8 mm.

input pin of Ectane and excited by a sinusoidal voltage of 10 V amplitude at a frequency of 100 kHz, the shielding plate and guard electrode were connected to the ground potential, and the sensing electrode was connected to the output pin of Ectane. Ectane was connected to the computer by a cable and the data acquisition system was controlled by Magnifi, which is the specific software designed for Ectane, to process. All experimental results were obtained by manual scan.

The experimental arrangement used for the capacitive technique experiments presented in this work is shown in Figure 15. The driving electrode was excited by a sinusoidal voltage of 10 V amplitude at a frequency of 100 kHz and the shielding plate and guard electrode are connected to the ground potential. In this experimental system, capacitive sensors were used to detect the defects buried in an acrylic board. As shown in Figure 16, the 25 mm thick non-conducting specimen (acrylic board) contained six buried defects and the six buried defects from left to right were abbreviated to D1, D2, D3, D4, D5, and D6. The diameter of

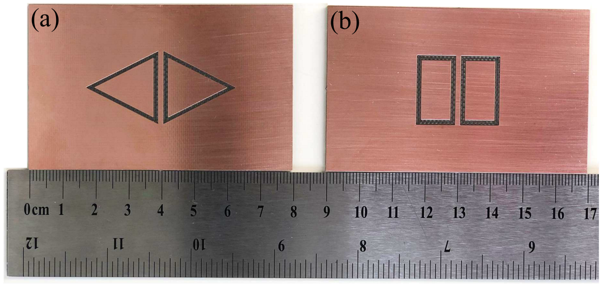

Figure 17: Two different shapes of the coplanar capacitive sensor with an equal area, equal separation distance, and equal close edge: (a) Triangular probe and (b) Rectangular probe.

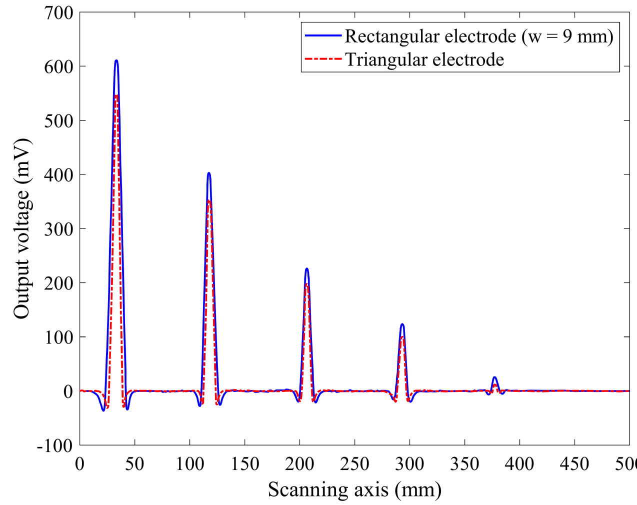

Figure 18: Experimental results showing output voltage with two different shapes of the coplanar capacitive sensor: Rectangular probe and Triangular probe with the equal area, equal separation distance, and equal close edge. The experiments were performed in 0.1 mm lift-off.

each of these six defects was 15 mm and they were located from left to right at depths of 1, 2, 3, 4, 6 and 8 mm, respectively. The distance between any centre of two adjacent defects was 90 mm. The red dash-line shown in Figure 16 was the inspection path using the capacitive sensors. Based on the simulation, to obtain the maximum penetration depth and electric field strength, a lift-off of 0.1 mm was considered in all experiments.

4. Experimental results and discussion

4.1. Different shape of the electrodes with the equal area

Two different shapes of coplanar electrodes with equal overall areas are used in this section to demonstrate the effect of these two electrode shapes on the sensor performance, as shown in Figure 17, namely a capacitive probe with back-to-back triangular electrodes (left side) and rectangular electrodes (right side). The sensor dimensions evaluated here are described in Figure 4. For the triangular electrodes, the geometry can be specified by the size of the base (b) = 18 mm, the height (h) = 18 mm, and the separation between the closest points of the two triangles (s) = 4.5 mm. For the rectangular electrodes, the geometry can be specified by the size of the length (l) = 18 mm, the width (w) = 9 mm, and the separation between the closest points of the two rectangles (s) = 4.5 mm.

The scan results over the hidden side of the defects which are shown in Figure 18 indicate that none of the probes could detect defect D6 which means both sensor shapes have the same sensing depth and this is because the closest edge of the driving and sensing electrode in both of them have the same size (l = b). However, the measured voltage of the pair of rectangular-shaped electrodes is higher. It can be inferred that the most important parts in the single pair capacitive sensors with the equal area of the electrodes and the same separation between electrodes are the closest two edges of the main electrodes which specify the output result. This result is in good qualitative agreement with the simulation conducted earlier.

4.2. The rectangular probe with different widths of the electrodes

In addition to the basic geometry of the probe, the probe performance is also determined by other parameters such as its size and the separation distance between the electrodes. To investigate the effect of the size of the coplanar electrodes on the sensor performance, three different widths of the rectangular electrodes were considered while the length and the separation between electrodes were kept constant. The width of the electrodes is 12, 9, and 6 mm, their length is 18 mm and the separation between them is 4.5 mm in each probe. The three capacitive sensors are denoted according to their size: LRE (Large rectangular electrode) when w = 12 mm, MRE (Medium rectangular electrode) when w = 9 mm, and SRE (Small rectangular electrode) when w = 6 mm. The dimension characteristics of these sensors are summarized in Table 1.

Considering the effects of the electrode width on the sensor performance results shown in Figure 19, for all three pairs of rectangular electrodes, the output voltage amplitude reduces with decreasing electrode width. The sensing depth

Table 1
Dimension characteristics of the three pairs of the rectangular probe with the different widths of the electrodes. LRE, MRE, and SRE refer to to Large rectangular electrode, Medium rectangular electrode, and Small rectangular electrode, respectively.

	l (mm)	w (mm)	s (mm)
LRE	18.0	12.0	4.5
MRE	18.0	9.0	4.5
SRE	18.0	6.0	4.5

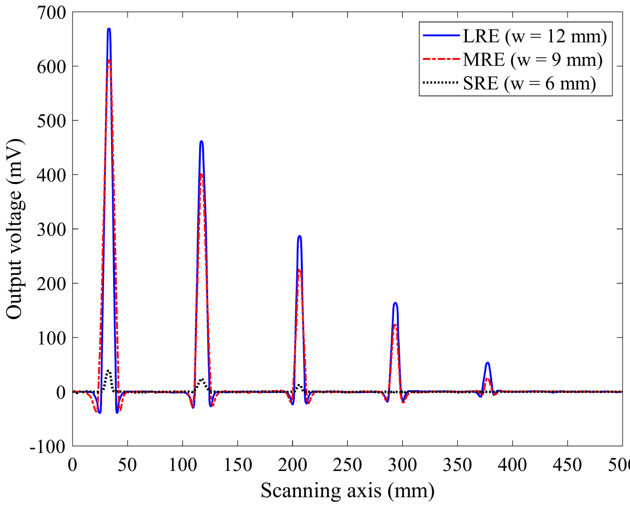

Figure 19: Experimental results showing output voltage with three different widths of the rectangular coplanar capacitive sensor: LRE (Large rectangular electrode) with w = 12 mm, MRE (Medium rectangular electrode) with w = 9 mm, and SRE (Small rectangular electrode) with w = 6 mm. The experiments were performed in 0.1 mm lift-off.

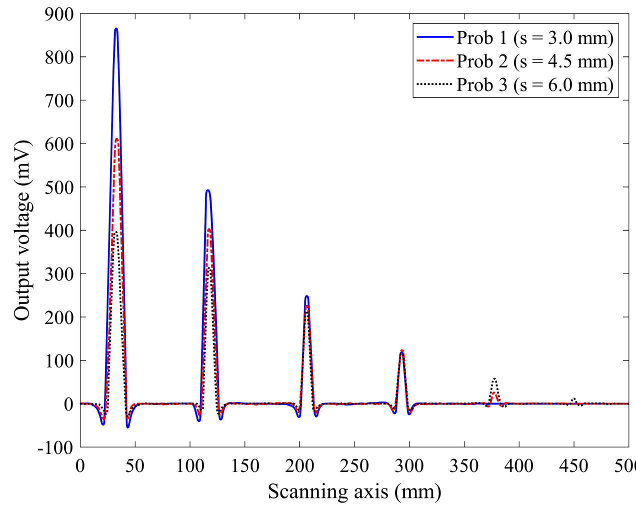

Figure 20: Experimental results showing output voltage with three different separations (3.0, 4.5, and 6.0 mm) of the rectangular coplanar capacitive sensor. The experiments were performed in 0.1 mm lift-off.

of LRE and MRE is almost the same (since none of them could detect D6) and greater than the sensing depth of SRE. It was expected that the sensing depth of the sensor would increase by increasing the electrode width and hence the electrode area, but this increase was not directly proportional which means the separation between the electrodes also has an impact on the sensing depth, as indicated in the numerical simulation and the next section.

4.3. The rectangular probe with different separation distances between electrodes

The separation distance between the electrodes is one of the other factors which affects the performance of the coplanar capacitive sensor. As might be expected, the voltage detected on the sensing electrode decreases as the separation between the two adjacent electrodes increases. Three different separations distances (3, 4.5, and 6 mm) of the rectangular probe were selected to study the effect of this parameter, while keeping the same overall electrode area. The dimension characteristics of these sensors are shown in Table 2.

The simulation section has indicated that a probe design with a larger separation distance between the two electrodes decreases the electric field strength as the field lines are spread over a larger volume of the sample, however, this gives a greater penetration depth into the specimen. The physical experiments confirm this result. From the experimental results in Figure 20, it can be seen that the penetration depth increases with the separation distance between the electrodes while the output voltage amplitude decreases. If the separation distance between the electrodes decreases, the coupling between them is stronger and the electric field lines will be more concentrated at the sample surface. Conversely, the greater distance between the electrodes leads to a weaker coupling between them and the electric field lines will be more prone to go further to reach the sensing electrode. This increases the penetration depth and is hence useful for the detection of deeper features. As is obvious, Probe 1 cannot detect D5 located at a depth of 6 mm, while Probe 2 and Probe 3 could easily detect this defect. In addition, Probe 3 detected D6 located at a depth of 8 mm. However, the measured voltage for Probe 3 is smaller than Probe 2, and the measured voltage for Probe 2 is smaller than Probe 1. Therefore, there is a trade-off between measured voltage and the penetration of the electric field into the specimen.

Table 2
Dimension characteristics of the three pairs of the rectangular probe with the different separation distances between the electrodes.

	l (mm)	w (mm)	s (mm)
Probe 1	18.0	9.0	3.0
Probe 2	18.0	9.0	4.5
Probe 3	18.0	9.0	6.0

4.4. Discussion

Figure 21 presents the summary of the experimental results based on the defect depth (mm) and output voltage (mV). According to the results in Figure 21 (a), for a rectangular probe with constant length and separation distance between the electrodes, the electrode with a larger width provides a higher output voltage and can reach a deeper penetration depth. Although the probe with w = 6 mm can detect the defect at a depth of 3 mm and less, the output voltage is much lower than the probe with w = 9 and 12 mm. This is because the size and separation distance between electrodes is small in comparison with the size of the defects (diameter of the

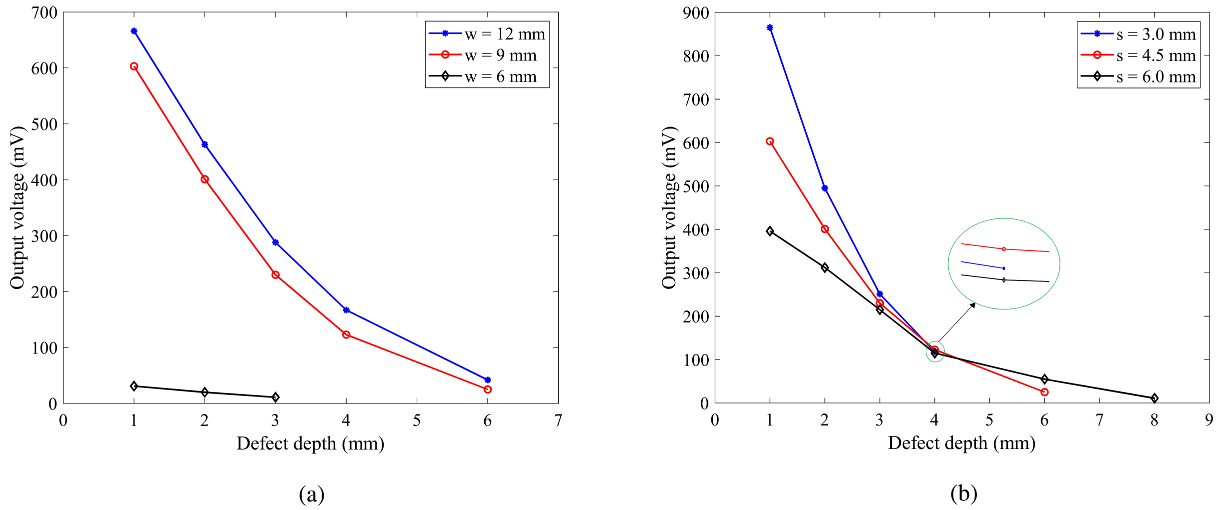

Figure 21: Summary of the experimental results: (a) the rectangular probe with l = 18, s = 4.5, and w = 12, 9, and 6 mm; (b) the rectangular probe with l = 18, w = 9, and s = 3.0, 4.5, and 6.0 mm.

defect = 15 mm). The two other probes can detect the defect at a depth of up to 6 mm. However, with w = 12 mm there will be a higher output voltage and hence, a higher signal to noise ratio.

In addition, increasing the separation between the electrodes will increase the penetration depth, however, causes a decrease in output voltage leading to a lower signal-to-noise ratio. From the results in Figure 21 (b), it can be inferred that for the rectangular probe with a constant length and width, the sensor with a 3 mm separation distance between the electrodes can be employed to detect the defect at a depth of 4 mm or less to achieve the maximum signal-to-noise ratio. To inspect the defect at a depth between 4 and 6 mm, the probe with s = 4.5 mm gives the best result, and likewise, the probe with s = 6 mm can be applied to detect the defect at a depth between 6 and 8 mm. Therefore, the coplanar capacitive sensor should be optimized based on the application and features of the inspected defect which is mentioned in the introduction. Furthermore, the size of the sensor and the defect must be in the same range and comparable to obtain the correct and desirable results.

Note that, the sensor design is based on the specimen type, its thickness, and the size of the defects. For a sample with a different thickness or material with a different relative permittivity, and different size/type of defect, there should be a compromise between the electrode size and the separation distance between them.

5. Conclusions

In this paper, the influences of design parameters such as shape/size/spacing, shielding plate and guard electrode on the performance of the coplanar capacitive sensor were studied based on numerical simulations and experimental investigations. In addition, the effect of the frequency and lift-off on the penetration depth and electric field strength were evaluated. The finite element modelling showed that frequency is not the main factor for evaluating the performance of a coplanar capacitive sensor and (within a limited range) has no significant impact on penetration depth, affecting electric field strength. A triangular and a rectangular probe were selected to study the impact of the electrode shape on the sensor performance. It was shown that both probes have the same penetration depth, however, the rectangular probe has a greater electric field strength and it is recommended when there is a space restriction. The effect of the presence or absence of the shielding plate and guard electrode, as well as the electrode size and separation distance, were considered through FEM for a rectangular probe. It was found that the presence of both the shielding plate and guard electrode increases the penetration depth but decreases the electric field strength. Furthermore, it was demonstrated that both the electric field strength and penetration depth increase by increasing the size of the coplanar electrodes. The sensing depth of the coplanar capacitive sensor increases with the increasing separation distance between the electrodes, while the electric field strength decreases as the coupling between the driving and sensing electrode will be weaker. Moreover, it is inferred that the lift-off should be minimized as much as possible in order to achieve greater output for a non-conducting sample.

The experimental results suggest that for both triangular and rectangular probes with an equal area of the electrodes and the same separation distance, the penetration depth is almost the same, but the measured output voltage of the rectangular shape electrode is greater than the triangular shape electrode. In order to demonstrate the impact of electrode size on the electric field strength and sensing depth, three different widths of the rectangular electrode were employed. It was observed that by increasing the electrode width, the measured output voltage amplitude increases as well as the penetration depth. In addition, the results of the experiments with three different separation distances of the rectangular probe showed that increasing the separation distance between the driving and sensing electrodes leads to increasing the penetration depth, while reducing the electric field strength. The experimental results demonstrated a good qualitative agreement with the numerical simulations.

In practice, the situation is usually rather more complicated compared to the sample studied in this work. Defect types and sizes will be unknown and may be poorly defined. Further development of the capacitive probe is needed to meet different practical requirements and provide enhanced diagnostic information, e.g. systematic identification and characterization of defects. The development of multi-electrode capacitive sensors would be one of such improvements that could provide more information on the defect properties. This type of capacitive sensor will be studied in future works.

Acknowledgement

The support of the NSERC CREATE-oN DuTy! Program is gratefully acknowledged. The authors would like to express their appreciation to Eddyfi Inc. and the Computer Vision and Systems Laboratory of Laval University for their continuous support. The authors would also like to thank Dr. Alireza Sadeghi Chahardeh and Dr. Annette Schwerdtfeger for the time they spent reviewing this article.

References

[1] S Gholizadeh. A review of non-destructive testing methods of composite materials. *Procedia Structural Integrity*, 1:50–57, 2016. https://doi.org/10.1016/j.prostr.2016.02.008.

[2] Tianming Chen. Capacitive sensors for measuring complex permittivity of planar and cylindrical structures. 2012. https://doi.org/10.31274/etd-180810-2654.

[3] GG Diamond, DA Hutchins, TH Gan, P Purnell, and KK Leong. Single-sided capacitive imaging for ndt. *Insight-Non-Destructive Testing and Condition Monitoring*, 48(12):724–730, 2006. https://doi.org/10.1784/insi.2006.48.12.724.

[4] Subhas C Mukhopadhyay. Novel planar electromagnetic sensors: Modeling and performance evaluation. *Sensors*, 5(12):546–579, 2005. https://doi.org/10.3390/s5120546.

[5] Zheng Liu and Huan Liu. Experimenting capacitive sensing technique for structural integrity assessment. In *2017 IEEE International Conference on Industrial Technology (ICIT)*, pages 922–927. IEEE, 2017. https://doi.org/10.1109/ICIT.2017.7915483.

[6] Xiaohui Hu and Wuqiang Yang. Planar capacitive sensors–designs and applications. *Sensor Review*, 2010. https://doi.org/10.1108/02602281011010772.

[7] Lasitha Piyathilaka, Basuru Sooriyaarachchi, Sarath Kodagoda, and Karthick Thiyagarajan. Capacitive sensor based 2d subsurface imaging technology for non-destructive evaluation of building surfaces. In *2019 IEEE International Conference on Cybernetics and Intelligent Systems (CIS) and IEEE Conference on Robotics, Automation and Mechatronics (RAM)*, pages 287–292. IEEE, 2019. https://doi.org/10.1109/CIS-RAM47153.2019.9095810.

[8] Xavier Dérobert, Jean Iaquinta, Gilles Klysz, and Jean-Paul Balayssac. Use of capacitive and gpr techniques for the non-destructive evaluation of cover concrete. *Ndt & E International*, 41(1):44–52, 2008. https://doi.org/10.1016/j.ndteint.2007.06.004.

[9] Farima Abdollahi-Mamoudan, Sebastien Savard, Tobin Filleter, Clemente Ibarra-Castanedo, and Xavier PV Maldague. Numerical simulation and experimental study of capacitive imaging technique as a nondestructive testing method. *Applied Sciences*, 11(9):3804, 2021. https://doi.org/10.3390/app11093804.

[10] X Yin and DA Hutchins. Non-destructive evaluation of composite materials using a capacitive imaging technique. *Composites Part B: Engineering*, 43(3):1282–1292, 2012. https://doi.org/10.1016/j.compositesb.2011.10.018.

[11] Subhas Chandra Mukhopadhyay and Chnithaka P Gooneratne. A novel planar-type biosensor for noninvasive meat inspection. *IEEE Sensors Journal*, 7(9):1340–1346, 2007. https://doi.org/10.1109/JSEN.2007.903335.

[12] Marc Genest, Dennis Krys, and Catalin Mandache. Capacitive sensing for the detection of tile misalignment in ceramic armor arrays. *NDT & E International*, page 102261, 2020. https://doi.org/10.1016/j.ndteint.2020.102261.

[13] Yunzhi Huang, Zheng Zhan, and Nicola Bowler. Optimization of the coplanar interdigital capacitive sensor. In *AIP Conference Proceedings*, volume 1806, page 110017. AIP Publishing LLC, 2017. https://doi.org/10.1063/1.4974695.

[14] Zhen Li, Xiaokang Yin, Yue Gu, Guoming Chen, and Wei Li. Discriminating the defects in the insulation layer and metal surface using multi-electrode capacitive sensor. *Review of Progress in Quantitative Nondestructive Evaluation*, 2019.

[15] Xiaokang Yin, David A Hutchins, Guoming Chen, and Wei Li. Detecting surface features on conducting specimens through an insulation layer using a capacitive imaging technique. *NDT & E International*, 52:157–166, 2012. https://doi.org/10.1016/j.ndteint.2012.08.004.

[16] Xiaokang Yin, Zhen Li, Wei Li, Guoming Chen, et al. Corrosion depth inversion method based on the lift-off effect of the capacitive imaging (ci) technique. *IEEE Access*, 8:22770–22779, 2020. https://doi.org/10.1109/ACCESS.2020.2970204.

[17] Yu Cheng, Su Diao, Asad Hanif, Pavithra Parthasarathy, and Zongjin Li. Development and application of a novel low-cost capacitive sensor for accurate rebar position detection. *Construction and Building Materials*, 257:119506, 2020. https://doi.org/10.1016/j.conbuildmat.2020.119506.

[18] Amr A Nassr, Wael H Ahmed, and Wael W El-Dakhakhni. Coplanar capacitance sensors for detecting water intrusion in composite structures. *Measurement science and technology*, 19(7):075702, 2008. https://doi.org/10.1088/0957-0233/19/7/075702.

[19] Maxim Morozov, William Jackson, and SG Pierce. Capacitive imaging of impact damage in composite material. *Composites Part B: Engineering*, 113:65–71, 2017. https://doi.org/10.1016/j.compositesb.2017.01.016.

[20] Xiaokang Yin, David A Hutchins, Guoming Chen, and Wei Li. Investigations into the measurement sensitivity distribution of coplanar capacitive imaging probes. *NDT & E International*, 58:1–9, 2013. https://doi.org/10.1016/j.ndteint.2013.04.001.

[21] Alexander V Mamishev, Kishore Sundara-Rajan, Fumin Yang, Yanqing Du, and Markus Zahn. Interdigital sensors and transducers. *Proceedings of the IEEE*, 92(5):808–845, 2004. https://doi.org/10.1109/JPROC.2004.826603.

[22] Farima Abdollahi, Sebastien Savard, Xavier Maldague, Tobin Filleter, and Hakim Bendada. Non-destructive testing of materials by capacitive sensing. In *3rd International Symposium on Structural Health Monitoring and Nondestructive Testing 25-26 Nov 2020, Quebec, Canada (NDT-SHM 2020)*, 2020. http://www.ndt.net/?id=25574.

[23] Dixiang Chen, Xiaohui Hu, and Wuqiang Yang. Design of a security screening system with a capacitance sensor matrix operating in single-electrode mode. *Measurement Science and Technology*, 22(11): 114026, 2011. https://doi.org/10.1088/0957-0233/22/11/114026.

[24] Xiaokang Yin, Chen Li, Zhen Li, Wei Li, and Guoming Chen. Lift-off effect for capacitive imaging sensors. *Sensors*, 18(12):4286, 2018. https://doi.org/10.3390/s18124286.

[25] Xiaokang Yin, David A Hutchins, Guoming Chen, Wei Li, and Zhiqian Xu. Studies of the factors influencing the imaging performance of the capacitive imaging technique. *Ndt & E International*, 60:1–10, 2013. https://doi.org/10.1016/j.ndteint.2013.07.001.

[26] Xiaokang Yin, David A Hutchins, Guoming Chen, and Wei Li. Preliminary studies on the design principles of capacitive imaging probes

for non-destructive evaluation. *International Journal of Applied Electromagnetics and Mechanics*, 42(3):447–470, 2013. https://doi.org/10.3233/JAE-131676.

[27] X Yin, GG Diamond, and DA Hutchins. Further investigations into capacitive imaging for nde. *Insight-Non-Destructive Testing and Condition Monitoring*, 51(9):484–490, 2009. https://doi.org/10.1784/insi.2009.51.9.484.

[28] Kefan Wang, Xiaokang Yin, Chen Li, Wei Li, and Guoming Chen. Capacitive imaging technique for the inspection of composite sucker rod. *Chinese Journal of Mechanical Engineering*, 32(1):1–11, 2019. https://doi.org/10.1186/s10033-019-0421-z.

[29] Xiaokang Yin, DA Hutchins, GG Diamond, and P Purnell. Non-destructive evaluation of concrete using a capacitive imaging technique: Preliminary modelling and experiments. *Cement and Concrete Research*, 40(12):1734–1743, 2010. https://doi.org/10.1016/j.cemconres.2010.08.015.

[30] https://www.lpkfusa.com/.

[31] Zhen Li, Guoming Chen, Yue Gu, Kefan Wang, Wei Li, and Xiaokang Yin. Further investigations into the capacitive imaging technique using a multi-electrode sensor. *Applied Sciences*, 8(11):2296, 2018. https://doi.org/10.3390/app8112296.